

Ultimate flexural strength of normal section of FRP-confined RC circular columns

Gu Dongsheng^{1, 2} Wu Gang² Wu Zhishen²

(¹College of Environment and Civil Engineering, Jiangnan University, Wuxi 214122, China)

(²Key Laboratory of Concrete and Pre-Stressed Concrete Structures of the Ministry of Education, Southeast University, Nanjing 210096, China)

Abstract: Numerical analysis is carried out to study the sectional properties of the fiber-reinforced polymer (FRP)-confined reinforced concrete (RC) circular columns. The axial load ratio, the FRP confinement ratio and the longitudinal reinforcement characteristic value are the three main parameters that can influence the neutral axis depth when concrete compression strain reaches an ultimate value. The formula for computing the central angle θ , corresponding to the compression zone, is established according to the data regression of the numerical analysis results. The numerical analysis results demonstrate that the concrete stress enhancement from transverse confinement and strain hardening of the longitudinal reinforcement can cause a much greater flexural strength than that defined by the design code. Based on the analytical studies and the test results of 36 large scale columns, the formula to calculate the flexural strength when columns fail under seismic loading is proposed, and the calculated results agree well with the test results. Finally, parametric studies are conducted on a typical column with different axial load ratios, longitudinal reinforcement characteristic value and FRP confinement ratios. Analysis of the results shows that the calculated flexural strength can be increased by 50% compared to that of unconfined columns defined by the code.

Key words: reinforced concrete (RC) circular columns; flexural capacity of normal section; fiber-reinforced polymer (FRP); confinement

Concrete columns designed and constructed without adequate confinement reinforcement in potential plastic hinge regions are particularly vulnerable in earthquakes. Therefore, retrofitting concrete columns is of paramount importance in the rehabilitation of existing structures. In recent years, fiber-reinforced polymer (FRP) jacketing has become a popular material to retrofit existing deficient columns. An extensive review of the literature shows that the behavior of FRP-confined concrete specimens under concentric loading conditions has been extensively studied. In contrast, a relatively limited number of studies have been reported on FRP-confined columns under simulated seismic loading^[1].

The main objective of this paper is to calculate the flexural strength of normal sections of FRP-confined reinforced concrete (RC) circular columns when columns fail under

seismic loading. The experimental flexural strength has been reported to be much greater than the flexural strength defined by the code^[2], which corresponds to a concrete compression strain of 0.003 3^[3]. This difference is because the concrete stress is enhanced by transverse confinement. In addition, the strain hardening of the longitudinal reinforcement also causes strength enhancement. This enhancement in flexural strength may be undesirable because it can cause shear force to increase. Thus, the enhancement in flexural strength should be properly considered and studied. Calculating the flexural strengths of RC circular columns is difficult because they need to be solved by trigonometric transcendental equations^[3], and FRP confinement increases this difficulty. This paper extensively studies this problem, and the effects of FRP confinement, axial load level, and longitudinal reinforcement strain hardening are properly considered.

1 Numerical Simulations

Numerical simulations, which are often used to investigate the cross-sectional behavior of concrete members^[4-5], are conducted to study the depth of the neutral axis in this section. Previous studies indicated that determining the depth of the neutral axis is the key problem in calculating the flexural strengths of circular columns. The layered representation of a section is used in the numerical simulations, as shown in Fig. 1(a). In the figure, R is the radius of a section; r_s is the distance from the center of the circle to the center of the longitudinal bar; and θ is half of the central angle corresponding to the compression zone. The confined concrete material properties account for the effect of FRP confinement. The longitudinal bar is also represented by layers with the appropriate material properties. The program calculates the moment-curvature response by incremental analysis based on the plane section hypothesis.

The model proposed by Lam and Teng^[6] is proved to be the most suitable for FRP-confined concrete, so it is adopted

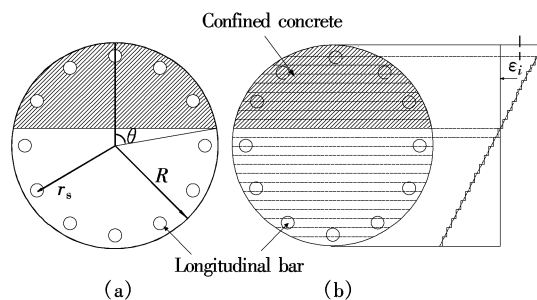


Fig. 1 Sectional analysis. (a) Sectional geometry; (b) Layered representation of a section

Received 2009-11-20.

Biographies: Gu Dongsheng (1978—), male, doctor, lecturer, gussds@yahoo.com.cn; Wu Gang (1976—), male, doctor, professor, g.wu@seu.edu.cn.

Foundation items: The National Basic Research Program of China (973 Program) (No. 2007CB714200), the National Natural Science Foundation of China (No. 50608015, 50908102).

Citation: Gu Dongsheng, Wu Gang, Wu Zhishen. Ultimate flexural strength of normal section of FRP-confined RC circular columns[J]. Journal of Southeast University (English Edition), 2010, 26(1): 107 – 111.

here for the numerical simulations. The tensile strength of the concrete is not considered. A uniaxial bilinear model is used for the stress-strain relationship of the longitudinal reinforcement, where the strain hardening modulus is 0.01 times the elastic modulus.

1.1 Parameters for numerical simulations

A typical bridge pier with a diameter of 1 m, a clear cover of 40 mm, and a cylinder compressive strength f'_c of 30 MPa is used for the analysis. The longitudinal reinforcement yield strength f_{yl} is 420 MPa. The conclusions derived are generalized by adopting non-dimensional parameters in the following study. The axial load ratio n , defined as $n = N/A_g f'_c$, where A_g is the gross cross-sectional area, varies from 0.1 to 0.4, incremented by 0.1. The longitudinal reinforcement ratio ρ_s ($\rho_s = A_s/A_g$, where A_s is the area of longitudinal reinforcement) changes from 1% to 4% with 1% increments. The corresponding longitudinal reinforcement characteristic values ($\lambda_l = \rho_s f_{yl}/f'_c$) are 0.14, 0.28, 0.42, and 0.56. Similar ranges in values for parameters are investigated in previous studies^[4]. The confinement ratio λ_f varies from 0.1 to 0.3 with increments of 0.1, where $\lambda_f = f_l/f'_c = 2E_f t_f \varepsilon_f / D f'_c$. Here f_l is the lateral confining pressure exerted by the FRP; E_f is the modulus of the FRP; t_f is the thickness of the FRP jacket; ε_f is the rupture strain of the FRP jacket; and D is the diameter of the sections.

1.2 Numerical results

The central angle θ , corresponding to the compression zone when the strain of the extreme compressive fiber reaches its ultimate strain, is the main concern in the numerical simulations. The calculated θ is plotted in Fig. 2. The results for θ given confinement ratios of only 0.1 and 0.3 are shown in the figure for brevity. From Fig. 2, the main factor that affects θ is the axial load ratio n , with the almost linear increase in θ with the increase in n . The effects of the FRP confinement ratio and the longitudinal reinforcement characteristic value on θ are also significant. The expression of θ can be proposed as

$$\theta = \frac{n}{a\lambda_l + b\lambda_f + c} + \frac{d\lambda_l + e\lambda_f + f}{a\lambda_l + b\lambda_f + c} \quad (1)$$

where a , b , c , d , e , and f are unknown parameters that can be obtained by data regression of the numerical simulation results. Linear regression of the numerical results, including 48 data points, leads to the following equation:

$$\theta = \frac{n + 1.56\lambda_l + 0.11\lambda_f + 0.20}{1.08\lambda_l + 0.34\lambda_f + 0.38} \quad (2)$$

Fig. 3 compares the calculated results from Eq. (2) with the numerical results; the calculated results agree well with the numerical results. The ratio of the calculated results from Eq. (2) to the numerical results has a mean of 1.0 and a coefficient of variation (COV) of 0.7%.

Fig. 4 displays how θ , calculated from Eq. (2), increases with the increase of longitudinal reinforcement characteristic values when the axial load is low. Under a high axial load, this increase is insignificant because θ is greater for the sec-

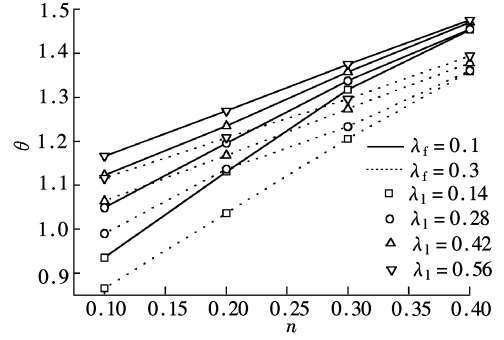


Fig. 2 Relationship between θ and n

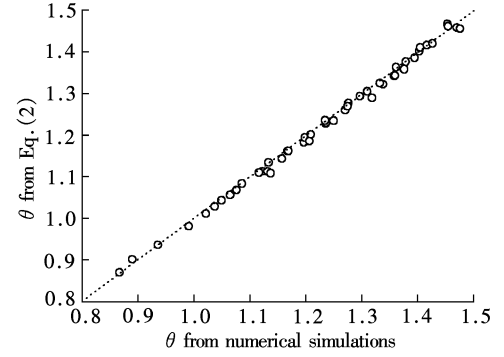


Fig. 3 Comparison of numerical simulation results with Eq. (2) for θ

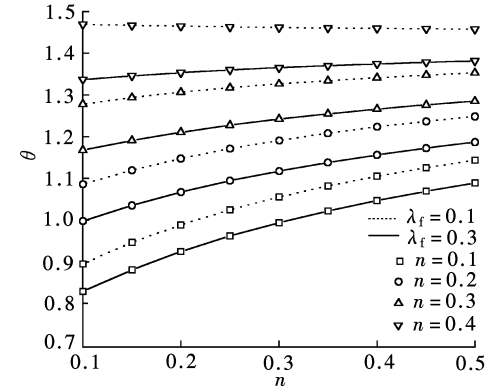


Fig. 4 Relationship between θ and the longitudinal reinforcement characteristic value

tion confined with less FRP than that confined with more FRP. This difference in θ is because the concrete stress is larger when the section is confined by more FRP, and the neutral axis depth is lower under the same axial load ratio.

2 Model of Flexural Strength

2.1 Expression of flexural strength

Flexural strength of a section can be computed by adding the moment of the forces about the tension reinforcement M_s to the moment M_n of the axial force. The moment of compression reinforcement is ignored because the value is minor compared with that of the tension reinforcement^[7]. We can compute M_s by assuming that the tension reinforcement is located at the centroid of the distributed reinforcing layer and reaches the yield strength. Geometrically, the distance from the centroid of the compression zone to the center of the circle is defined as $r_1 = 4R \sin^3 \theta / (6\theta - 3 \sin 2\theta)$. The distance from the centroid of the distributed tension reinforcing

layer to the center of the circle is defined as $r_2 = r_s \sin(\pi - \theta) / (\pi - \theta)$. When calculating M_s , the length of the lever arm is $r_1 + r_2$; when calculating M_n , the length of the lever arm is r_1 . M_s and M_n can be expressed as

$$M_s = \left(1 - \frac{\theta}{\pi}\right) f_{yl} A_s \left[\left(r_s \frac{\sin(\pi - \theta)}{\pi - \theta} \right) + 4R \frac{\sin^3 \theta}{6\theta - 3\sin 2\theta} \right] \quad (3)$$

$$M_n = n f'_c \pi R^2 \frac{4R \sin^3 \theta}{6\theta - 3\sin 2\theta} \quad (4)$$

Substituting the expression for λ_1 for brevity, M_u can be expressed as

$$M_u = M_s + M_n = f'_c \pi R^3 \left\{ \lambda_1 \left(1 - \frac{\theta}{\pi}\right) \left[\left(\frac{r_s}{R} \frac{\sin(\pi - \theta)}{\pi - \theta} \right) + \frac{4\sin^3 \theta}{6\theta - 3\sin 2\theta} \right] + n \frac{4\sin^3 \theta}{6\theta - 3\sin 2\theta} \right\} \quad (5)$$

2.2 Comparison with experimental data

To validate the equations previously developed, test re-

sults reported in the literature for FRP-confined circular columns under simulated seismic loading are collected. Tests are screened according to the following criteria: 1) The columns should be flexure-critical, and the failure mode is controlled by rupture of the FRP at the base of the column; 2) There is no lap splice in the plastic hinge region; 3) Fibers of the FRP are in the lateral direction. A total of 36 FRP-confined circular columns meet the above criteria. Tab. 1 provides details of these collected columns. Because little lateral steel reinforcement is used in all of the columns, confinement by steel reinforcement is not considered. The second order effect of axial load is considered when determining the measured M_u listed in Tab. 1.

Calculated values for θ from Eq. (2) and M_u from Eq. (5) are listed in Tab. 1. Calculated M_u values are relatively smaller than measured values because when calculating M_u , the longitudinal reinforcement stress is assumed to be equal to the yield strength. Reports have shown that reinforcement at the extreme tension fiber may fracture when confined columns

Tab. 1 Details of test specimens

Specimen	D/mm	f'_c/MPa	f_{frp}/MPa	λ_f	d_b/mm	f_{yl}/MPa	λ_1	n	θ	$M_u/(\text{kN}\cdot\text{m})$		
										Measured	Eq. (5)	Eq. (7)
Cs-csj-rt ^[8]	610	36	552	0.38	19	303	0.16	0.06	0.81	650	580.4	652.2
Cs-Isj-rt ^[8]	610	36	552	0.51	19	303	0.16	0.06	0.78	645	588.5	657.2
ST2NT ^[9]	356	40	1 896	0.14	25	500	0.37	0.64	1.73	270	260.4	320.9
ST3NT ^[9]	356	41	1 896	0.11	25	500	0.36	0.64	1.75	278	256.7	317.2
ST4NT ^[9]	356	45	1 896	0.11	25	500	0.33	0.31	1.34	269	281.6	336.4
ST5NT ^[9]	356	41	1 896	0.07	25	500	0.36	0.31	1.36	267	264.9	320.2
FCS-1 ^[10]	760	19	4 170	0.24	19	426	0.43	0.17	1.15	1 754	1 287.5	1 560.1
FCS-2 ^[10]	760	19	4 170	0.16	19	426	0.43	0.17	1.18	1 700	1 265.4	1 543.2
RC1 ^[11]	270	90	3 800	0.21	16	500	0.16	0.31	1.25	198	192.5	213.9
RC2 ^[11]	270	75	3 800	0.12	16	500	0.19	0.34	1.35	160	166.1	188.5
RC3 ^[11]	270	50	3 800	0.19	16	500	0.28	0.52	1.58	140	132.8	156.7
C60n1 ^[12]	180	59	3 430	0.43	12	353	0.16	0.43	1.32	52	45.0	49.6
C60n2 ^[12]	180	59	3 430	0.43	12	353	0.16	0.52	1.46	64	45.7	50.6
C60n3 ^[12]	180	77	3 430	0.33	12	353	0.12	0.43	1.37	63	52.4	57.1
C80n1 ^[12]	180	77	3 430	0.33	12	353	0.12	0.52	1.52	72	52.3	57.3
C80n2 ^[12]	180	77	3 430	0.33	12	353	0.12	0.62	1.67	73	49.7	54.8
C80n3 ^[12]	180	59	3 430	0.43	12	353	0.16	0.62	1.59	68	44.6	49.7
CSR-1 ^[13]	610	41	4 168	0.22	19	299	0.14	0.05	0.82	635	575.9	647.4
CSR-2 ^[13]	610	39	4 430	0.25	19	299	0.15	0.06	0.82	650	574.8	646.8
CSR-3 ^[13]	610	44	415	0.32	19	481	0.21	0.05	0.86	945	813.9	935.5
CSR-4 ^[13]	610	44	1 245	0.11	19	481	0.21	0.05	0.92	940	788.9	919.9
Fig. 7 ^[14]	180	48	1 400	0.14	13	604	0.53	0.11	1.15	56	45.5	56.4
Fig. 8 ^[14]	180	48	1 400	0.14	13	604	0.53	0.48	1.52	68	52.2	65.3
Fig. 9 ^[14]	180	48	1 400	0.72	13	604	0.53	0.11	1.01	59	49.7	59.5
Fig. 10 ^[14]	180	48	1 400	0.72	13	604	0.53	0.48	1.32	83	62.7	74.9
Fig. 11 ^[14]	180	48	1 400	0.43	13	604	0.53	0.48	1.41	71	57.9	70.6
Fig. 13 ^[14]	180	48	1 500	0.15	13	604	0.53	0.11	1.15	51	45.6	56.5
Fig. 15 ^[14]	180	48	1 500	0.77	13	604	0.53	0.11	1.00	57	50.0	59.7
ACTT 9513 ^[15]	610	44	911	0.17	19	293	0.17	0.05	0.86	803	677.2	773.3
ACTT 9519 ^[16]	610	38	1 006	0.16	19	289	0.19	0.05	0.89	803	647.0	745.5
CG2 ^[17]	300	25	1 214	0.22	12	416	0.31	0.20	1.15	119	90.9	107.3
CH2 ^[18]	360	35	1 832	0.19	25	380	0.63	0.36	1.39	420	337.8	423.9
CH3 ^[18]	360	35	3 945	0.16	25	380	0.63	0.36	1.40	452	334.8	421.2
CL4 ^[18]	360	35	1 832	0.30	25	380	0.63	0.36	1.36	396	348.3	433.1
CL5 ^[18]	360	35	3 945	0.26	25	380	0.63	0.36	1.37	444	344.8	430.0
CL6 ^[18]	360	35	3 945	0.37	25	380	0.63	0.36	1.34	465	354.2	438.3

fail under seismic loading^[1]. Thus, the extreme tension reinforcement stress should be observably greater than the yield strength. To consider this effect, M_s from Eq. (3) needs modification. The reinforcement tension stress and the compression stress are closely related to the neutral axis depth and θ . The relationship between θ and the ratios of calculated M_s to measured M_s , obtained by subtracting M_n calculated from Eq. (4) from the measured M_u , is presented in Fig. 5. Linear regression of their relationship can be expressed as

$$\zeta = 1.05 - 0.24\theta \quad (6)$$

where ζ is the ratio of the calculated M_s to the measured M_s . To correctly calculate M_s , Eq. (3) can be divided by ζ , so M_u can be modified by

$$M_u = f'_c \pi R^3 \left\{ \frac{\lambda_1}{1.05 - 0.24\theta} \left(1 - \frac{\theta}{\pi} \right) \left[\left(\frac{r_s}{R} \frac{\sin(\pi - \theta)}{\pi - \theta} \right) + \frac{4\sin^3\theta}{6\theta - 3\sin 2\theta} \right] + n \frac{4\sin^3\theta}{6\theta - 3\sin 2\theta} \right\} \quad (7)$$

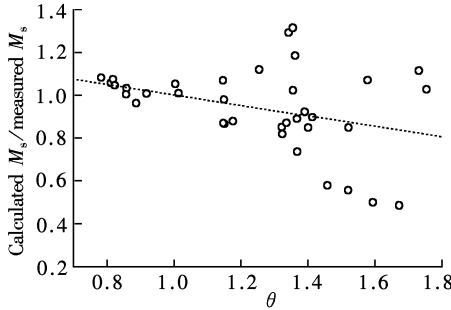


Fig. 5 The relationship between θ and the ratio of calculated M_s to measured M_s

Fig. 6 displays the values of M_u calculated from Eq. (7) and the measured M_u values in the form of the non-dimensional parameter $M_u/\pi R^3 f'_c$. The ratios of the calculated results to the test results have a mean value of 0.99 and a COV of 12.3%; the calculated results agree well with the measured results.

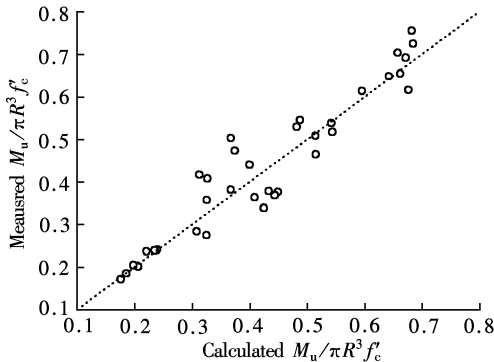


Fig. 6 Comparison of calculated M_u to measured M_u

3 Parametric Studies

Parametric studies are performed to gain a general understanding of the effect that various design parameters have on M_u given by Eq. (7). The moment enhancement ratio, which is the ratio of M_u divided by the flexural strength M_i

defined by the code, of unconfined columns is discussed to study the effect of FRP confinement. M_i is the flexural strength when the extreme compressive strain of concrete reaches 0.0033. A prototype bridge column with a diameter equal to 600 mm is selected for the parametric studies. The thickness of the concrete cover is 25 mm. The diameter of the longitudinal reinforcement is assumed to be 19 mm with a yield strength of 400 MPa. The concrete cylinder compressive strength is 36 MPa. The calculated moment enhancement ratio is presented in Fig. 7 for columns with an axial load level of 0.1 and 0.5 with different longitudinal reinforcement characteristic values. The moment enhancement ratio always increases with the increase in the axial load ratio, which agrees well with conclusions from previous studies^[2]. The moment enhancement ratio is more significant for the section confined with more FRP when other parameters are kept constant. Under high axial load, the moment enhancement ratio is 1.5 when the FRP confinement ratio is 0.3. This moment enhancement should be adequately considered when calculating shear forces of confined columns under seismic loading.

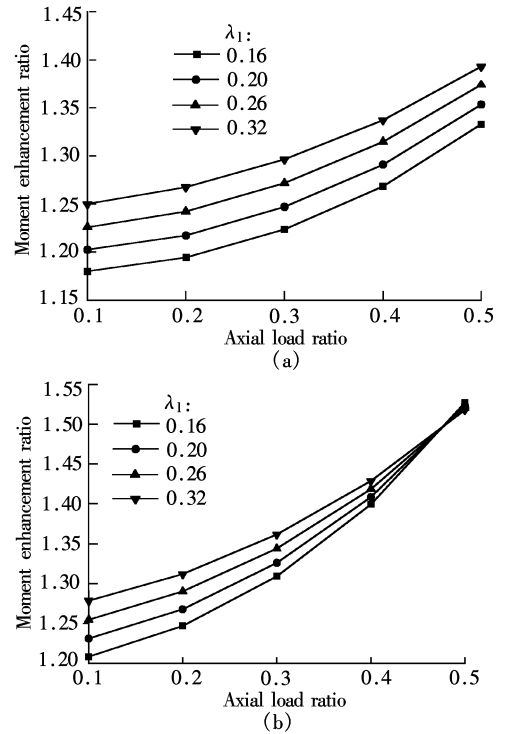


Fig. 7 Moment enhancement ratio vs. axial load ratio. (a) $\lambda_f = 0.1$; (b) $\lambda_f = 0.3$

4 Conclusions

By combining numerical simulations, analytical studies and regression analyses using a test database, which includes data obtained from the authors' own tests and data collected from the literature, simple expressions are developed for calculating the flexural strength of FRP-confined circular columns. The following conclusions are drawn:

1) Numerical simulation results show that the axial load ratio, the FRP confinement ratio and the longitudinal reinforcement characteristic value are the three main parameters that can influence the depth of the neutral axis. Based on

the regression of the numerical analysis results, the formula for computing the central angle θ , corresponding to a compression zone, is established.

2) The analytical model demonstrates how the flexural strength is significantly affected by the FRP confinement ratio, the axial load level, and the longitudinal reinforcement characteristic value when columns fail under seismic loading. The ratios of calculated results to test results of 36 larger scale columns have a mean value of 0.99 and a COV of 12.3%.

3) Parametric studies show how the flexural strength can be 1.5 times that of unconfined columns defined by the code when FRP-confined circular columns fail under seismic loading. This moment enhancement should be adequately considered when calculating the shear force of confined columns under seismic loading.

References

- [1] Wu Yufei, Liu Tao, Oehlers D J. Fundamental principles that govern retrofitting of reinforced concrete columns by steel and FRP jacketing [J]. *Advanced Structural Engineering*, 2006, **9**(4): 507–533.
- [2] Priestley M J N, Park R. Strength and ductility of concrete bridge columns under seismic loading [J]. *ACI structural Journal*, 1987, **84**(1): 61–76.
- [3] Ministry of Construction of the People's Republic of China. Chinese code for design of concrete structures GB50010—2002[S]. Beijing: China Architecture and Building Press, 2002. (in Chinese)
- [4] Kowalsky M J. Deformation limit states for circular reinforced concrete bridge columns [J]. *Journal of Structural Engineering ASCE*, 2000, **126**(8): 869–878.
- [5] Paultre P, Légeron F. Confinement reinforcement design for reinforced concrete columns [J]. *Journal of Structural Engineering ASCE*, 2008, **134**(5): 738–749.
- [6] Lam L, Teng J G. Design-oriented stress-strain model for FRP-confined concrete [J]. *Construction and Building Materials*, 2003, **17**(6/7): 471–489.
- [7] Binici B. Design of FRPs in circular bridge column retrofits for ductility enhancement [J]. *Engineering Structures*, 2008, **30**(3): 766–776.
- [8] Xiao Y, Wu H, Martin G R. Prefabricated composite jacketing of RC columns for enhanced shear strength [J]. *Journal of Structural Engineering ASCE*, 1999, **125**(3): 255–264.
- [9] Sheikh S A, Yau G. Seismic behavior of concrete columns confined with steel and fiber-reinforced polymers [J]. *ACI Structural Journal*, 2002, **99**(1): 72–81.
- [10] Li Y F, Sung Y Y. A study on the shear-failure of circular sectioned bridge column retrofitted by using CFRP jacketing [J]. *Journal of Reinforced Plastics and Composites*, 2004, **23**(8): 811–830.
- [11] Ozbakkaloglu T, Saatcioglu M. Seismic behavior of high-strength concrete columns confined by fiber-reinforced polymer tubes [J]. *Journal of Composites for Construction*, 2006, **10**(6): 538–549.
- [12] Wang Zhenyu, Lu Xuelei, Li Wei, et al. Experimental research on seismic performance of high strength concrete circular column confined with carbon fiber sheets at plastic hinge zone [J]. *Building Structure*, 2009, **39**(2): 21–24. (in Chinese)
- [13] Haroun M A, Elsanadedy H M. Behavior of cyclically loaded squat reinforced concrete bridge columns upgraded with advanced composite-material jackets [J]. *Journal of Bridge Engineering*, 2005, **10**(6): 741–748.
- [14] Gould N C, Harmon T G. Confined concrete columns subjected to axial load, cyclic shear, and cyclic flexure—Part II: experimental program [J]. *ACI Structural Journal*, 2002, **99**(1): 42–50.
- [15] Seible F, Hegemier G A, Priestley M J N, et al. Fiberglass shell jacket retrofit test of a circular shear column with 2.5% reinforcement. Report No. ACTT-95/13 [R]. San Diego: The University of California, San Diego, 1995.
- [16] Innamorato D, Seible F, Hegemier G A, Priestley M J N. Carbon shell jacket retrofit test of a circular shear column with 2.5% reinforcement. Report No. ACTT-95/19 [R]. San Diego: The University of California, San Diego, 1995.
- [17] Dong Xuhua. Research on seismic behavior of reinforced concrete bridge short columns strengthened with GFRP [D]. Changsha: College of Civil Engineering of Hunan University, 2006. (in Chinese)
- [18] Gu Dongsheng, Wu Gang, Wu Zhishen, et al. Research of failure modes and fiber strain response of FRP-confined RC circular columns [J]. *World Information on Earthquake Engineering*, 2008, **24**(2): 60–67. (in Chinese)

FRP 加固 RC 圆柱正截面受弯承载力计算

顾冬生^{1,2} 吴 刚² 吴智深²

(¹ 江南大学环境与土木工程学院, 无锡 214122)

(² 东南大学混凝土及预应力混凝土结构教育部重点实验室, 南京 210096)

摘要: 运用数值计算方法对 FRP 加固钢筋混凝土 (RC) 圆柱截面特性进行计算, 发现截面破坏时受压区高度主要受轴压比、FRP 约束强度比和纵筋配筋特征值 3 个主要参数影响。根据数值计算的结果进行回归, 提出了受压区对应圆心角 θ 的计算方法。数值计算结果显示, 横向约束导致的混凝土应力提高以及纵筋屈服后的强化效应使 RC 柱破坏时截面受弯承载力远大于规范规定值。根据理论分析和 36 个大比例试件实测结果提出截面破坏时受弯承载力计算方法, 计算结果与试验结果吻合很好。最后, 对一个典型柱变形能力进行参数分析, 研究轴压比、纵筋配筋特征值和 FRP 约束强度比对正截面受弯承载力的影响。结果显示 FRP 加固圆柱破坏时受弯承载力可以比规范规定的未加固柱受弯承载力提高 50% 左右。

关键词: 钢筋混凝土圆柱; 正截面受弯承载力; 纤维增强复合材料; 约束

中图分类号: TU375.3